Received 28 June 2007
Revised 22 December 2007
Accepted 28 January 2008

Shape modification of an axial flow turbine nozzle to reduce erosion

Zdzislaw Mazur, Rafael Campos-Amezcua and Alfonso Campos-Amezcua
Instituto de Investigaciones Eléctricas, Cuernavaca, Morelos, México

Abstract

Purpose – This paper aims to validate an axial turbine modified nozzle design, looking for a reduction of the nozzle erosion process during operation in power plants.
Design/methodology/approach – The approach taken is numerical simulation using the computational fluid dynamics (CFD) tool, comparing original and proposed/modified nozzle designs.
Findings – The paper provides information about how to achieve a solution of the turbine operational problem (abrasive wear) by an analysis of flow patterns under a variety of conditions.
Research limitations/implications – It does not give a detailed interpretation of flow behaviour due to the lack of validation data.
Practical implications – A very useful flow simulation methodology that can be used in industry is provided.
Originality/value – The proposed design modification of an axial turbine nozzle with the aid of CFD simulation has not been performed yet. This paper investigates the possibility of nozzle erosion reduction by modifying local flow patterns.
Keywords Simulation, Fluid dynamics, Erosion, Turbines, Numerical analysis
Paper type Technical paper

Nomenclature

a	Speed of sound (m/s)
A_{face}	Surface area (m^2)
$C(d_p)$	Function of particle diameter
C_D	Drag coefficient
$C_{1\varepsilon}, C_{2\varepsilon}$	Constants
C_μ	Constant
d	Particle diameter (m)
$f(a)$	Impact angle function
F_x	Virtual mass force (N)
k	Turbulent kinetic energy (m^2/s^2)
$\dot{m}$	Mass flow (Kg/s)
M_t	Turbulent Mach number
p	Pressure (Pa)
R	Gas constant
$\vec{R}_{accretion}$	Accretion ratio (kg/m^2s)
$\vec{R}_{erosion}$	Erosion ratio (kg/m^2s)
Re	Reynolds number
s	Particle path (s)
S_{ij}	Mean rate-of-strain tensor ($s^{-1)}$
S	Modulus of the mean rate-of-strain tensor S_{ij} $S \equiv \sqrt{2S_{ij}S_{ij}}$ (s^{-1})
t	Time (s)
T	Integral time scale (s)
u	Velocity (m/s)
x	Distance co-ordinate (m)

Greek symbols

α	Impact angle of the particle (rad)

International Journal of Numerical Methods for Heat & Fluid Flow
Vol. 19 No. 2, 2009
pp. 242-258

0961-5539
DOI 10.1108/09615530910930991

α_k	Inverse effective Prandtl number for (k)	μ_{mol}	Molecular viscosity (Pas)
α_ε	Inverse effective Prandtl number for ϵ	ρ	Density (kg/m^3)
β	Logarithmic particle Reynolds number	ω	Angular velocity (rad/s)
γ	Ratio of specific heats (c_p/c_v)	*Subscripts*	
ε	Turbulent dissipation rate (m^2/s^3)	P	Particle
η_0	Constant	0	Initial condition
μ_{eff}	Effective viscosity (Pas)	1	Final condition
		F	Fluid

Introduction

Particle-laden fluids are responsible for costly erosion problems that reflect directly on the life of steam turbine components. Solid particle erosion (SPE) of steam turbine components, such as nozzles, blades, radial spill – strips, and control valves, has been a problem of concern to utilities for many years. Erosion damage is caused by oxide scale exfoliation from boiler tubes and/or steam leads which become entrained in the steam flow to the turbine, causing erosion of steam path components. In 300 MW capacity steam turbines, SPE damages the nozzle vane partition (Figure 1) reducing nozzle life significantly. Also, erosion arouses an increase in throat area through the nozzles and efficiency loss in the turbine. When throat area increases the turbine demands increased vapor flow to maintain power supply, and the system requires increased fuel supply, provoking an increase in pollutant emissions. This situation is significant and has forced power plant management to look for nozzle improvement methods to accomplish their service life extension. computational fluid dynamics (CFD) analysis has been considered as an effective tool since many nozzle configurations can be investigated at a low price and without costly experimentation (De Palma, 2006; Kassab *et al.*, 2003).

The key to understanding erosion is a detailed knowledge of coupled and complex fluid/solids interactions (Mitter *et al.*, 2004; Habib *et al.*, 2005). Because of experimental difficulties, solids motion studies are not common. Motion-picture, photographic

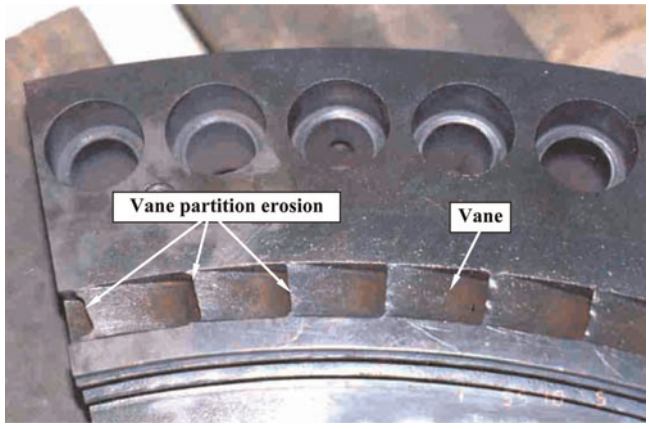

Figure 1.
Nozzle segment SPE damage

techniques, "quasi-stereoscopic" techniques and fiber-optic probes have been used (Lyczkowski and Bouillard, 2002) to determine particles velocity and size, but these techniques have some uncertainty, are tedious and time consuming or are intrusive, which may alter the flow field. An improved non-intrusive, radioactively tagging facility, the computer-aided particle tracking facility, has been used to obtain time-average solids motion features in fluidized beds (Lin *et al.*, 1995; Lyczkowski *et al.*, 1996). State-of-the-art CFD techniques and improved computing capabilities have made it possible to model the movement of solids in fluids (Ling *et al.*, 2003; Sundaresan *et al.*, 2003; Sommerfeld, 2003; Ciampini *et al.*, 2003; Bergeron and Vincent, 1999). The state-of-the-art of erosion modeling in fluid/solid systems was provided recently (Lyczkowski Bouillard, 2002). To be successful, fluid mechanics and erosion models must be used together; however, the coupling of fluid mechanics and erosion models is fairly recent (Tabakoff, 1990). Tabakoff has been engaged in turbine blade erosion and particulate flow research from 1971 to 1991. He developed a steady-state computer program capable of describing three-dimensional particle trajectories through turboaxial or radially rotating turbomachinery. He also obtained experimentally data on the restitution coefficient (the ratio of rebound to approach velocities) and the ratio of rebound to impingement angle by use of high-speed photography or laser Doppler anemometry expressed in terms of impingement angle. These ratios are used to account for the momentum loss of particles caused by collision with turbine blades or channel walls in the Lagrangian trajectory calculation. Tsuji (2000) carried out discrete particle simulation using instantaneous time dependent particle velocities. Direct numerical simulation of fluidized particles was developed by Joseph (2001). This method requires no adjustable parameters and appears to be truly predictive if the number of particles can be made sufficiently large. Chen *et al.* (1998) proposed a general impact friction model (computational mean particle erosion model) which characterizes the rise and decline of the friction coefficient with time and describes variations of the friction coefficient plateau level with the impact angle. This model is effective in explaining erosion rates obtained by experiments. The review of analytical and semi-empirical/empirical models of material removal for abrasive processes is presented by Neelesh and Vijaay (2001), including their limitations and applicability. Wang and Rajurkar (1996) and Lee and Chan (1997) developed abrasive particle material removal models based on the combined effects of impact indentation and fracture phenomena. These models can be used for brittle materials. Pei and Perreira (1998) and Paul *et al.* (1998) developed models for the ductile mode of material removal by plastic flow. These models are applicable only for ductile materials. Choi and Choi (1997) and Jain *et al.* (1999) proposed analytical models for the material removal of brittle and ductile materials based on the formation and propagation of micro-cracks (brittle materials) and plastic flow, i.e. ploughing action of abrasive particles (ductile materials).

Improvements in hydrodynamic models together with improvements in the erosion models presented herein enhanced the capabilities of analytical models to predict and estimate erosion rates in reasonable agreement with available erosion data.

There exists a consensus that the erosion process depends on the particle impingement angle, particle velocity and composition, as well as the kind of wall material (Curran, 1983; Franco and Roberts, 1998; Quercia *et al.*, 2001; Derevich, 2000). Particle impact angle and velocity play a main role on the erosion rate (Curran, 1983; Franco and Roberts, 1998). Thus, under these bases, any reduction of particle velocity

and particle impact angle on the wall below about 60° will in principle lead to an effective reduction of erosion, according to Curran (1983).

One of the economic ways to achieve a solution to the erosion problem (abrasive wear) is an analysis of the flow patterns within the turbine under a variety of conditions using the CFD technique as a tool. CFD can be used as an aid towards redesigning internal parts of the turbine.

The abrasive process on a surface is determined by relative velocity and particle impact angle as well as particle/steam flow ratio (Keck *et al.*, 1997). Particle motion is governed by local flow patterns. As flow patterns change significantly within a turbine, there is no possibility to predict abrasive wear without knowledge of local flow patterns.

It is considered that the main contribution of this paper consists of providing a flow simulation methodology that can be used in industry, which shows how to achieve a solution of equipment operational problems (SPE damage) applying an analysis of local flow pattern by means of CFD. The methodology provided makes it possible to modify local flow patterns and some flow parameters which results in effective erosion reduction.

Methodology

SPE damage of steam turbine nozzles (turbine control stage stationary blades) was observed to be concentrated at the nozzle vane partition section, as shown in Figure 1. The maximum erosion rate was registered at the vane trailing edge zone.

Flow simulation by means of CFD represents a way to understand local flow patterns in regions of high erosion damage, before suggesting any modification to the current design. Once the flow pattern is known, modifications to nozzle geometry could be suggested and then evaluated using the same CFD tool.

The particular objective of this paper is to study flow through the nozzle, for both current and proposed designs, looking for a reduction of the erosion process due to changes of particle trajectories, their velocity and impingement angle (angle of particle impact). Current nozzle design is composed of 56 vanes of convex/concave profile grouped in four segments. The proposed design consists of a step profile (1 mm off-set) forming on the nozzle concave side adjacent to the vane trailing edge. The 1 mm off-set step profile was chosen considering limitation of the vane trailing edge thickness which must be kept within design limits to avoid blade vibration and strength reduction. Prior to the last solution, several step profiles were tried in order to get maximum possible off-set from points of view of blade mechanical strength (calculations were made) and erosion, considering the above-mentioned limitation. The trailing edge region is kept without any changes comparing with the original design, and the pressure surface (concave side) is raised outwards into the channel. As a result of this blade profile change, the nozzle throat area, degree of reaction, blade life and dynamic performance (vibration) are not affected. It is estimated that the modified blade aerodynamic performance may be affected, but not significantly by separated flow and undercut in the trailing edge zone. On the other hand, an increase in the throat area through the nozzles due to erosion, together with the related efficiency losses is much bigger and more significant for turbine performance.

In the proposed design nozzle, flow is separated from the vane surface in the maximum erosion rate zone and as a result, the particle abrasion effect is reduced. Namely, the design proposed in this work allows for flow patterns with changes in particle trajectories, impinging on the nozzle surface, compared with the current design.

Computational model

Numerical three-dimensional predictions have been carried out with the finite volume code Fluent V6.0.12 using an Renormalization Group (RNG) *k–ϵ model* for turbulence (Mack *et al.*, 1999; Fluent V6.0.12, 2001). The RNG k–ϵ model is derived from instantaneous Navier–Stokes equations, using a rigorous mathematical technique called RNG methods. The analytical derivation results in a model with constants different from those in the standard k–ϵ model, and additional terms and functions in the transport equations for k and ϵ. The momentum equations derived from RNG theory are:

$$\frac{\partial}{\partial t}(\rho u_i) + \frac{\partial}{\partial x_j}(\rho u_i u_j) = \frac{\partial}{\partial x_j}\left[\mu_{eff}\left(\frac{\partial u_i}{\partial x_j} + \frac{\partial u_j}{\partial x_i}\right)\right] - \frac{\partial p}{\partial x_i} \tag{1}$$

The effective viscosity is computed using the high-Reynolds-number form of equation (2):

$$\mu_{eff} = \mu_{mol}\left[1 + \sqrt{\frac{C_\mu}{\mu_{mol}}}\frac{k}{\sqrt{\varepsilon}}\right]^2 \tag{2}$$

with $C\mu = 0.0845$.

The transport equations for k and ε provided by the RNG theory are:

$$\frac{\partial}{\partial t}(\rho k) + \frac{\partial}{\partial x_i}(\rho \mu_i k) = \frac{\partial}{\partial x_i}\left(\alpha_k \mu_{eff}\frac{\partial k}{\partial x_i}\right) + \mu_t S^2 - \rho\varepsilon\left(1 + 2M_t^2\right) \tag{3}$$

where $M_t = \sqrt{\frac{k}{a^2}}, a\left(\equiv \sqrt{\gamma RT}\right)$

$$\frac{\partial}{\partial t}(\rho\varepsilon) + \frac{\partial}{\partial x_i}(\rho\mu_i\varepsilon) = \frac{\partial}{\partial x_i}\left(\alpha_\varepsilon \mu_{eff}\frac{\partial \varepsilon}{\partial_i}\right) + C_{1\varepsilon}\frac{\varepsilon}{k}\mu_t S^2 - C_{2s}\rho\frac{\varepsilon^2}{k} - \frac{C_\mu \rho \eta^3(1-\eta/\eta_0)}{1+\beta\eta^3}\frac{\varepsilon^2}{k} \tag{4}$$

where $\eta \equiv Sk/\varepsilon, \eta_0 \approx 4.38, \beta = 0.012, C_{1\varepsilon} = 1.42, C_{2\varepsilon} = 1.68$.

In this work, the method used to account for particle erosion is based on calculations of the path of several solid particles through the flow field, the so-called Lagrangian tracking method. Each particle represents a sample of particles that follow an identical path. The tracked particle motion is taken to describe the average behavior of the dispersed phase.

While setting up Lagrangian tracking and erosion models as described below, the following assumptions have been made:

- particle – particle interactions are neglected;
- any change of flow turbulence caused by particles is not accounted for;
- only spherical, non-reacting and non-fragmentating particles are considered; and
- geometry modifications, caused by wall removal by solid particles, have been neglected. This means that the computational model geometry during simulation was invariable.

Governing equations

Consider a discrete particle traveling in a continuous fluid medium where the forces acting on the particle, which affect its acceleration, take place due to the difference in velocity between particle and fluid and also due to fluid displacement by the particle. The motion equation for this case was derived by Basset (1888) and Boussinesq (1897) for a stationary reference frame:

$$m_p \frac{dv_p}{dt} = 3\pi\mu d C_D\left(v_f - v_p\right) + \frac{\pi d^3 \rho_f}{6}\frac{dv_f}{dt} + \frac{\pi d^3 \rho_f}{12}\left(\frac{dv_f}{dt} - \frac{dv_p}{dt}\right) + F_x + \frac{3}{2}d^2\sqrt{\pi\rho_f\mu}\int_{t_0}^{t_1}\frac{\frac{(dv_f)}{(dt')} - \frac{(dv_p}{dt'})}{\sqrt{t-t'}}dt' - \frac{\pi d^3}{6}\left(\rho_p - \rho_f\right)\omega \times \left(\omega \times \vec{R}\right) - \frac{\pi d^3 \rho_p}{3}\varpi \times v_p \quad (5)$$

where F_x is the virtual mass force and is given by:

$$F_x = \frac{1}{2}\frac{\rho}{\rho_p}\frac{d}{dt}(v - v_p)$$

The last two terms of equation (5) are the centripetal and Coriolis forces, which are present only in rotating frames of reference. These two forces are not present under real operation conditions of the current steam turbine nozzle case. Thus, they are not included in the analysis. Since the steam flow in the nozzle region is not rotating like the nozzle does, centripetal and Coriolis forces are neglected. A drag coefficient C_D is introduced (Basset, 1888; Boussinesq, 1897) to account for experimental results on the viscous drag of a solid sphere. It depends on the particle Reynolds number. Within the range $0.01 < Re_p < 260$, the drag coefficient is given by the relations [Fluent V6.0.12, 2001]:

$$C_D = 1 + 0.1315(Re_p)^{0.82-0.05\beta} \quad Re_p < 20, \quad (6)$$

$$C_D = 1 + 0.1935(Re_p)^{0.6305} \quad Re_p > 20,$$

With $\beta = \log(Re_p)$, where the particle Reynolds number is defined by:

$$Re_p = \frac{\rho_f \left|v_f - v_p\right| d}{\mu} \quad (7)$$

If all particle acceleration terms are only on the left-hand side, the equations are integrated by a forward Euler integration method.

In turbulent flows, particle trajectories are not deterministic and two particles injected at a single point at different times may follow separate trajectories due to the random nature of the instantaneous fluid velocity. As a consequence, the particles disperse because of the fluctuating component of the fluid velocity. To account for the influence of turbulent fluid fluctuations on particle motion, the method originally

developed by Dukowicz (1980), Gosman and Ioannides (1983) and Faeth (1987) have been applied in the code.

Particle dispersion due to turbulence in the fluid phase is predicted using the stochastic tracking (random walk) model which includes the effect of instantaneous turbulent velocity fluctuations on particle trajectories using instantaneous values of the fluctuating gas flow velocity (equation 8) in the trajectory equations (equation 5), along the particle path during integration.

$$u = \bar{u} + u'(t) \tag{8}$$

In Fluent, the Discrete Random Walk model, or "eddy lifetime" model is used. In this model, fluctuating velocity components are discrete piecewise constant functions of time. Their random value is kept constant over an interval of time given by the characteristic lifetime of the eddies. Prediction of particle dispersion makes use of the integral time scale, T, concept which describes the time spent in turbulent motion along the particle path, ds:

$$T = \int_0^\infty \frac{u_p'(t)u_p'(t+s)}{\bar{u}_p'^2} ds \tag{9}$$

Integral time is proportional to the particle dispersion rate, as larger values indicate more turbulent motion in the flow. For small "tracer" particles that move with the fluid (zero drift velocity), the integral time becomes the fluid Lagrangian integral time, T_{L}. This time scale is approximated in the k-ε model as:

$$T_L \approx 0.15 \frac{k}{\varepsilon} \tag{10}$$

Data recorded during Lagrangian particle tracking are:

- the number of particles impinging on the surface;
- impinging velocity; and
- particle direction relative to the surface.

The removal of wall material is calculated using the Finnie (1960) model developed for ductile materials. Finnie derived the first model that describes erosive cutting by a single-particle. The major assumption is that a particle, approaching the eroding surface at angle α as measured from the surface (called the impingement angle), will remove material in much the same way as a machine tool would. The particle is assumed to be much harder than the surface and does not break up. The surface material is assumed to deform plastically during the cutting process; hence, the material is ductile. Ductile materials, such as aluminum or structural steel, can develop relatively large tensile strengths before they rupture.

It was assumed that there is:

- no thermophoretic force;
- no Brownian motion;
- no Saffman hit force; and
- no radiation heat transfer.

The change of continuous particles trajectory due to the effect of discrete phase trajectories on the continuum is also considered.

It is necessary to specify:

- the starting position and velocity for each particle stream (relative velocities if moving frames are used);
- particle diameter;
- the particle stream mass flow rate that will follow the trajectory of an individual particle/droplet $\dot{m}_p$ (required only for coupled calculations);
- that the injection refers to a stream of particles: single – one particle stream; group – more than one stream (initial conditions);
- the surface injection – or release particles from a surface previously defined at the steam stream entry.

In this case, a particle stream will be released from each facet of the surface. In order to avoid the use of too many particles, sample points in the plane surface are used.

In this work, surface injection was applied using sample points in the plain surface.

Particle erosion and accretion rates are monitored at wall boundaries. The erosion rate is defined as (Fluent V6.0.12, 2001):

$$R_{erosion} = \sum_{p=1}^{N_{particles}} \frac{\dot{m}_p C(d_p) f(\alpha)}{A_{face}} \tag{11}$$

Where $C(d_p)$ is a function of particle diameter, α is the particle path impact angle on the wall face, $f(\alpha)$ is the impact angle function and A_{face} is the wall face surface area. The accretion rate is defined as (Fluent V6.0.12, 2001):

$$R_{accretion} = \sum_{p=1}^{N_{particles}} \frac{\dot{m}_p}{A_{face}} \tag{12}$$

The computational domains that contain the details of both current and suggested steam turbine nozzle geometries are represented by two grids, which were used for conducting the investigation (Figure 2).

Geometric construction and meshing were performed with GAMBIT applying hexahedron cells. Both grids are non-structured with built in body fitted coordinates and have a number of 12,312 cells, 39,648 faces and 15,722 nodes (current design) and 12,456 cells, 40,110 faces and 15,897 nodes (suggested design), respectively. The y^+ value near the wall for the mesh is $y^+ = 5$. The mesh independence of numerical solution was checked. Prior to the last model, several meshes were tried in order to get grid independency of the solution. This was achieved by increasing the mesh resolution until sufficient accuracy was obtained.

As shown in Figure 2(b), the computational model of the proposed nozzle design has a modified profile/step profile (1 mm off-set) on the vane partition concave side adjacent to the vane trailing edge.

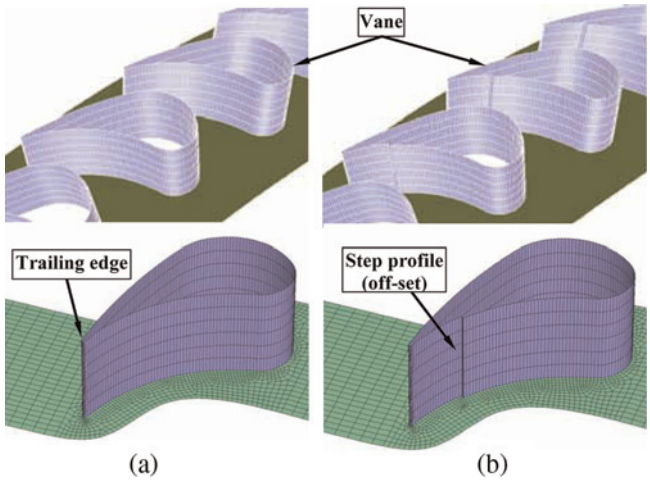

Figure 2.
Computational mesh for the nozzle: (a) current geometry and (b) proposed geometry

Boundary conditions

For the current simulation, particle diameter has been set to 100 m, based on a microscopic analysis of particles in steam. Boundary conditions were fixed from a set of initially calculated flow conditions, which were obtained by using the thermal balance of the unit. The thermal balance initial conditions of the units were as follows: steam pressure of 16.54 MPa, steam temperature of 537.8°C, steam mass-flow of 907,200 kg/h. A mass-flow inlet boundary was used for the incoming steam flow with mass-flow rate of 252 kg/s, temperature of 532.4 °C, and pressure of 15.72 MPa. The nozzle steam flow maximum Reynolds number is 4.18×10^7 and the maximum Mach number is 0.615. Turbulence intensity was fixed to $I = 5$ per cent after carrying out several trials according to Fluent (2001) and the turbulence length scale, $L = D_H = 0.0464$ m, based on hydraulic diameter of the steam path area. Calculations were started with turbulence intensity of 5 per cent and then values of 1 and 10 per cent were tried to see how much the solution varied. Finally, a value of 5 per cent was chosen because it was better suited for the current application considering nozzle flow Reynolds number. Turbulence intensity is defined as the ratio of RMS flow velocity fluctuations to the mean flow velocity. On the basis of different measurements and experiments in internal turbulent flows (tubes, turbine flow channels, closed internal channels), turbulence intensity does not typically exceed 15-20 per cent (Derevich, 2000; Johansson, *et al.*, 2003; Mendoza and Zhou, 2001). Because inflow velocity magnitudes are not known *a priori*, it is in these circumstances necessary to prescribe the local levels of turbulent kinetic energy, k, indirectly, by setting the local turbulence intensity, I.

This practice ensures that k, and turbulent viscosity, μ_t, will all scale correctly with u, which is desirable from both physical realism and a numerical stability point of view. A complete description about the effect of turbulence intensity on flow characteristics can be found in (Derevich, 2000; Johansson *et al.*, 2003; Mendoza and Zhou, 2001; Butler *et al.*, 2001). A pressure outlet boundary was determined as 11.22 MPa from a thermal balance of the unit. The particles/steam flow volume ratio was fixed at 0.025 (2.5 per cent). The nozzle vane material was martensitic stainless steel while the particle material was considered as oxide scale.

The no-slip condition was used in all the walls, and the velocity in the laminar sub-layer was calculated using the laminar stress-strain relationship.

Results

Modeling results

A converged solution was obtained using the turbulence RNG k-ε model after 6,850 iterations for the current configuration, while the solution for the proposed (modified) configuration required 7,340 iterations. The convergence of residuals for continuity, κ and ε were resolved to levels of 1E-3 while the energy equation was set to a level of 1E-6.

A series of results is presented, which compile the simulation carried out with current and proposed (with step profile/off-set) steam turbine nozzle configurations. All calculations were carried out with the turbine operating at steady-state conditions with nominal output of 300 MW.

Figure 3 shows the numerical solution for the current configuration in the form of two-dimensional contours of velocity in the nozzle flow channel on the nozzle vane transversal section in the cutting plane at 50 per cent height.

In Figure 4, a three-dimensional flow line path contours for the current nozzle design is presented, whereas Figure 5 shows two-dimensional flow velocity contours for modified nozzle geometry and Figure 6 flow line path contours for the same geometry. All numerical solutions presented are for the same comparable conditions.

Velocity contours for the current design (Figure 3) indicate that maximum flow velocity (390 m/s) is located in the nozzle throat and near to the vane trailing edge at the vane partition concave section where erosion damage is present. Figure 4(a) shows three-dimensional flow line contours for the current nozzle design and Figure 4(b) two-dimensional flow line contours (particle tracks zoom) for the same nozzle. In the proposed design case (Figure 5), the velocity contours show slightly lower (about 6.7 per cent) flow velocity on the nozzle surface, in the same nozzle throat zone (maximum velocity of 364 m/s), which is a result of the vane step profile.

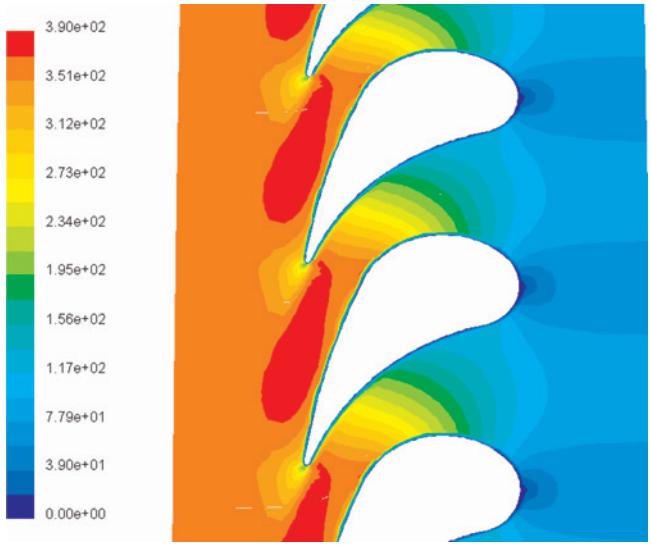

Figure 3.
Two-dimensional flow velocity contours for the current nozzle geometry (m/s) on the nozzle vane transversal section in the cutting plane at 50 per cent height

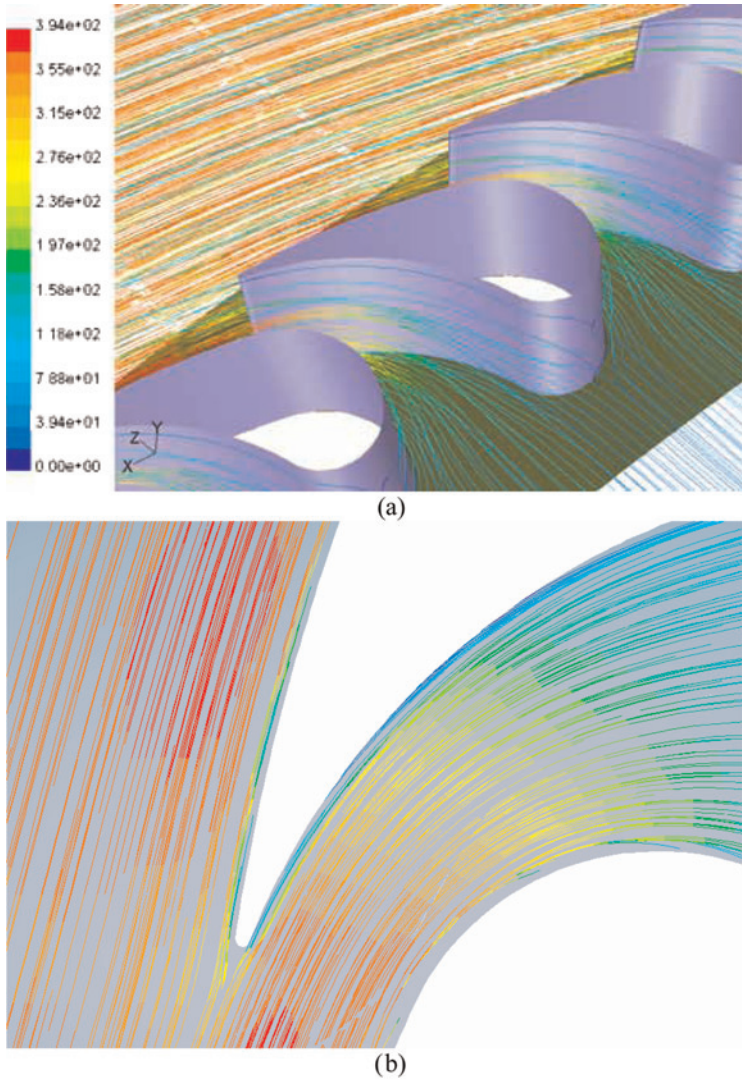

Figure 4.
Flow line path contours for the current nozzle design (m/s)

Notes: (a) Three-dimensional flow line path contours and (b) Two-dimentional flow line path contours (particles tracks zoom) on the nozzle vane transversal section in the cutting plane at 50 per cent height

The main difference between the current and proposed configurations is in the outer flow layer on the nozzle vane concave surface adjacent to the vane trailing edge. The present configuration is marked by flow concentration close to the vane wall (Figure 4).

The opposite situation was created in the proposed nozzle configuration (Figure 6). Due to the step profile (1 mm off-set) forming on the vane partition concave section the flow is separated from the vane surface in the maximum erosion rate zone. To estimate the influence of this situation on the nozzle erosion rate, solid particle trajectories were

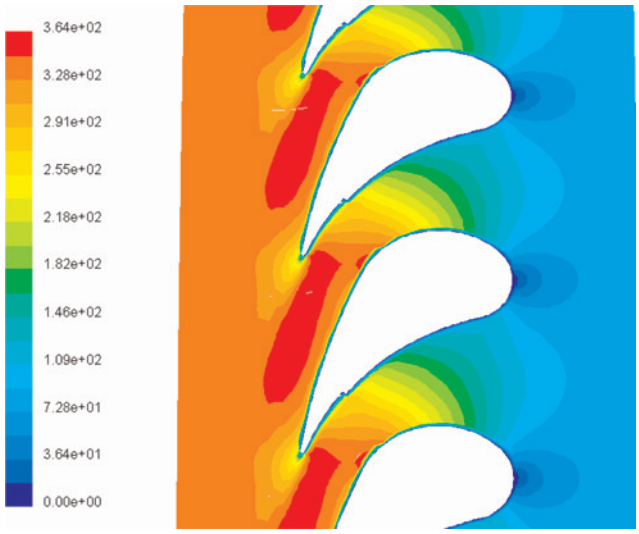

Figure 5.
Two-dimensional flow velocity contours for the modified/proposed nozzle geometry (m/s) on the nozzle vane transversal section in the cutting plane at 50 per cent height

simulated for the current nozzle design (Figure 4) and the modified nozzle design (Figure 6).

SPE reduction

The numerical results presented in the previous section have been used to estimate the steam turbine nozzle erosion rate with the current and proposed configurations (with step profile). During numerical simulation, 1,380 particles are tracked which are ejected in 138 points on the plain surface at the steam stream entry (at each point ten particles).

It is known (Curran, 1983; Keck, 1997) that one of the main parameters which influences erosion rate is particle impingement angle and particle velocity. From this knowledge, it is argued that the current physical nozzle arrangement facilitates nozzle partition section erosion. Erosion contours for the current nozzle geometry are presented in Figure 7.

The maximum erosion rate of 1.28 kg/m^{2}s was determined to be concentrated on the vane trailing edge at the vane partition concave section.

This is in good agreement with the nozzle erosion damage registered in the turbine, as previously shown in Figure 1. To calculate erosion rate from equation (11), the particle diameter dependency coefficient $C(d_p)$ was set to =1 because the particle diameter was fixed as invariant during the simulation ($d = 100$ m) and the impact angle dependency function f(α) was used as (Finnie, 1960):

$$f(\alpha) = \sin(2\alpha) - 3\sin^2(\alpha) \quad \text{for} \quad \alpha \leq 18.43^\circ \tag{13}$$

and

$$f(\alpha) = \cos^2(\alpha)/3 \quad \text{for} \quad \alpha > 18.43^\circ \tag{14}$$

As a result, the erosion rate units are mass of material removed per unit area and time. Similar erosion contours on the proposed nozzle geometry (with step profile/off-set) are presented in Figure 8.

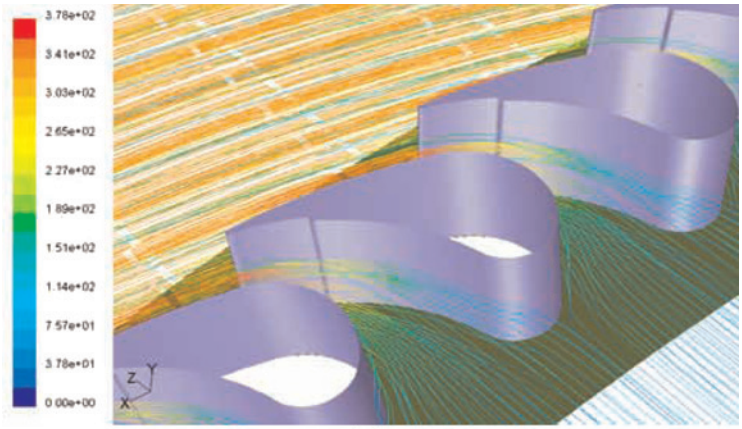

(a)

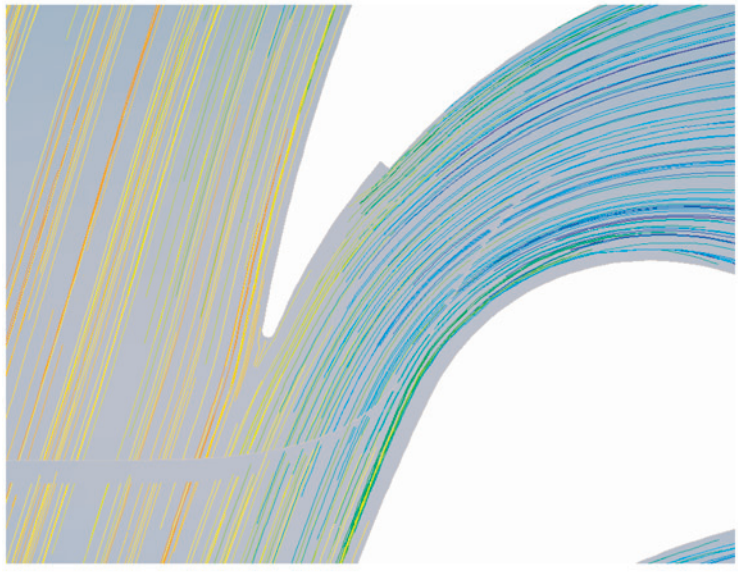

(b)

Notes: (a) Three-dimensional flow line path contours and (b) Two-dimentional flow line path contours (particles tracks zoom) on the nozzle vane transversal section in the cutting plane at 50 per cent height

Figure 6.
Flow line path contours for the modified/proposed nozzle design (m/s)

In this case, the predicted nozzle erosion damage is distributed more uniformly on the nozzle vane surface and the maximum erosion rate was determined to be 0.643 kg/m^{2}s. This means that predicted nozzle erosion rate was reduced by 50 per cent compared to the original nozzle design and is due to particle trajectory changes, reduced particle velocity and particle impingement angle changes (nozzle design modification).

As is shown in Figure 9, particles coming from the region near pressure surface are separated from the vane after passing step profile formed close to the trailing edge. Due to this situation, particle impact density on the vane partition near to the trailing

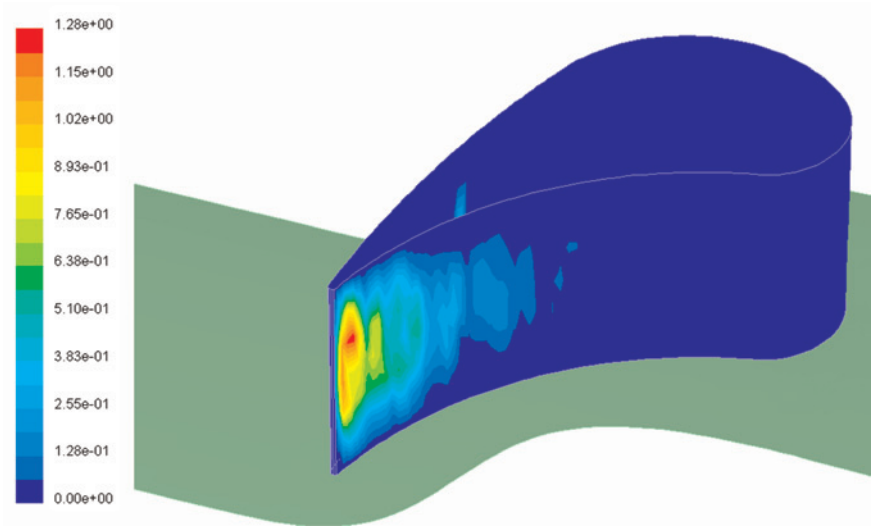

Figure 7.
Three-dimensional erosion rate contours on the current nozzle geometry (kg/m^{2}s)

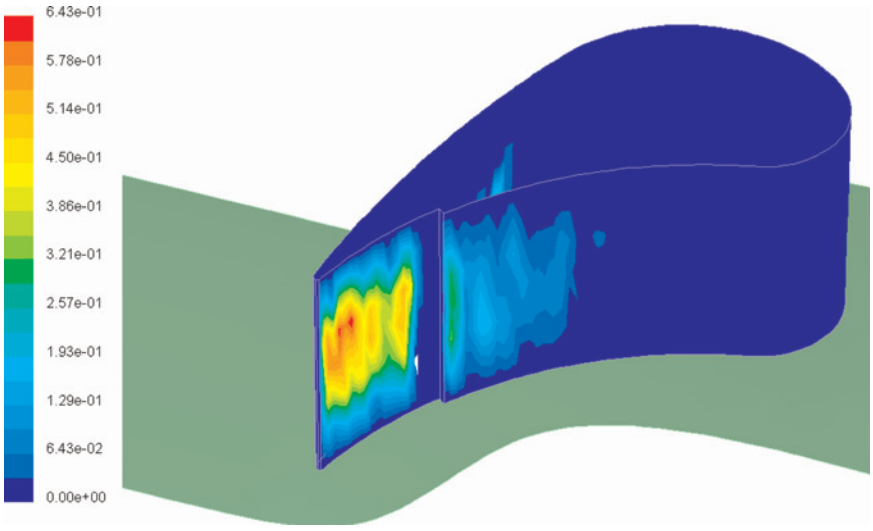

Figure 8.
Three-dimensional erosion rate contours on the modified/proposed nozzle geometry (kg/m^{2}s)

edge is reduced because fewer particles are impacting the vane surface. Also, particles impact angle on the vane partition is reduced provoking a decrease of erosion rate.

Based on this result, it was found that the time between nozzle maintenance for replacement/repair may be extended over 100 per cent using the new nozzle configuration design for vane profile. In this investigation, total blade surface erosion was not estimated.

Conclusions

A three-dimensional fluid-flow simulation and the prediction of SPE based on the Lagrangian particle tracking method for a 300 MW steam turbine nozzle (control stage stationary blades), which is reported to be affected by erosion have been presented. The erosion process depends strongly on particle trajectories, particle velocity and particle

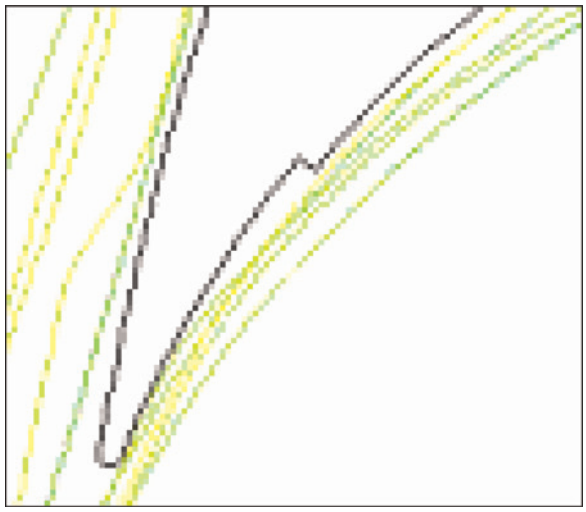

Figure 9.
Two-dimensional flow line path contours (particles tracks zoom) on the modified nozzle vane transversal section.

angle of impact (impingement angle). Modifications to nozzle geometry design have has been analyzed by changing nozzle vane geometry (step profile/off-set) which results in solid particle modified trajectory and impingement angle. Predictions showed that an effective 50 per cent reduction of nozzle erosion rate is achieved with the proposed design. This, in turn, renders a 100 per cent extended time between nozzle maintenance or replacement, indicating a significant benefit of the proposed design on nozzle life. Results also show that numerical simulation can really be used in a predictive manner. Simulation results can serve as an input in an early stage of the design procedure to determine modified system parameters and increase component life-time. In order to validate the results discussed in this paper, it is planned to include the redesigned steam turbine nozzle proposed here in a forthcoming overhaul of the current operating unit.

References

Basset, A.B. (1888), *Hydrodynamics*, Cambridge University Press, London.

Bergeron, S. and Vincent, A. (1999), "Implementation strategies for real-time particle transport solver", *Computer Physics Communications*, Vol. 120, pp. 177-84.

Boussinesq, J. (1897), *Théorie de L'écoulement Tourbillonmant et Tumultueux des Liquids, Dans les Lits Rectilignes á Grandes Sections*, Comptes Rendus de l'Académie des Sciences, Paris.

Butler, R.J., Byerley, A.R., Treuren, K.V. and Baughn, J.W. (2001), "The effect of turbulence intensity and length scale on low-pressure turbine blade aerodynamics", *International Journal of Heat and Fluid Flow*, Vol. 22, pp. 123-33.

Chen, D., Sarumi, M. and Al-Hassani, S.T.S. (1998), "Computational mean particle erosion model", *Wear*, Vol. 214, pp. 64-73.

Choi, G.S. and Choi, G.H. (1997), "Process analysis and monitoring in abrasive water jet machining of alumina ceramics", *International Journal of Machine Tools and Manufacture*, Vol. 37, pp. 295-307.

Ciampini, D., Spelt, J.K. and Papini, M. (2003), "Simulation of interference effects in particle streams following impact with a flat surface", *Wear*, Vol. 254, pp. 237-49.

Curran, R.E. (1983), *Solid Particle Erosion Turbulent Design and Materials*, Technical Report No. CS-3178, EPRI, Palo Alto, CA.

De Palma, P. (2006), "Numerical simulations of the three-dimensional transitional compressible flows in turbomachinery cascades", *International Journal of Numerical Methods for Heat and Fluid Flow*, Vol. 16, pp. 509-29.

Derevich, I.V. (2000), "Statistical modeling of mass transfer in turbulent two-phase dispersed flows", *International Journal of Heat and Mass Transfer*, Vol. 34, pp. 243-152.

Dukowicz, J.K. (1980), "A particle-fluid numerical model for liquid sprays", *Journal of Computational Physics*, Vol. 35 No. 5, pp. 229-53.

Faeth, G.M. (1987), "Mixing, transport and combustion in sprays", *Progress in Energy and Combustion Science*, Vol. 13 No. 12, pp. 293-345.

Finnie, J. (1960), "Erosion of surfaces by solid particles", *Wear*, Vol. 3 No. 46, pp. 87-103.

Fluent V6.0.12 (2001), *User's Guide*, Vol. 3, Fluent Incorporated, Lebanon.

Franco, A. and Roberts, S.G. (1998), "The effect of impact angle on the erosion rate of polycrystalline α-Al_2O_3", *Journal of The European Ceramic Society*, Vol. 6, pp. 123-32.

Gosman, A.D. and Ioannides, E. (1983), "Aspects of computer simulation of liquid-fueled combustors", *Journal of Energy*, Vol. 7 No. 32, pp. 482-90.

Habib, M.A., Ben-Mansour, R., Badr, H.M., Said, S.A.M. and Al-Anizi, S.S. (2005), "Erosion in the tube entrance region of a shell and tube heat exchanger", *International Journal for Numerical Methods for Heat and Fluid Flow*", Vol. 15, pp. 143-60.

Jain, R.K., Jain, V.K. and Dixit, P.M. (1999), "Modeling of material removal and surface roughness in abrasive flow machining process", *International Journal of Machine Tools and Manufacture*, Vol. 39, pp. 1903-23.

Johansson, B., Ljus, C. and Almstedt, A.E. (2003), "Application of wedge-shaped hot-film probes in a gas-particle flow", *Experimental Thermal and Fluid Science*, Vol. 45, pp. 112-21.

Joseph, D.D. (2001), "Lift correlations from direct numerical simulation of solid-liquid flow", *Proceedings of Fourth International Conference on Multiphase Flow, San Diego, CA, paper no. 385*.

Kassab, A., Divo, E., Heidmann, J., Steinthorsson, E. and Rodriguez, F. (2003), "BEM/FVM conjugate heat transfer analysis of a three-dimensional film cooled turbine blade", *International Journal of Numerical Methods for Heat and Fluid Flow*, Vol. 13, pp. 581-610.

Keck, H., Drtina, P. and Sick, M. (1997), "Flow computation in the whole turbine", *Sulzer Technical Review*, Vol. 22 No. 1, pp. 26-9.

Lee, T.C. and Chan, C.W. (1997), "Mechanism of ultrasonic machining of ceramic composites", *Journal of Materials and Processing Technology*, Vol. 71, pp. 95-201.

Lin, J.S., Chen, M.M. and Chao, B.T. (1995), "A novel radioactive particle tracking facility for measurement of solids motion in fluidized beds", *AIChE Journal*, Vol. 3 No. 31, pp. 465-73.

Ling, J., Skurdanov, P.V., Lin, C.X. and Ebadian, M.A. (2003), "Numerical investigation of liquid-solid slurry flows in a fully developed turbulent flow region", *International Journal of Heat and Fluid Flow*, Vol. 43, pp. 287-94.

Lyczkowski, R.W. and Bouillard, J.X. (2002), "State-of-the-art review of erosion modelling in fluid/solids systems", *Progress in Energy and Combustion Science*, Vol. 28, pp. 543-602.

Lyczkowski, R.W., Gamwo, I.K., Dobran, F. *et al.* (1996), "Validation of computed solids hydrodynamics and pressure oscillations in a model bubbling atmospheric fluidized bed combustor", *Powder Technology*, Vol. 76 No. 1, pp. 65-77.

Mack, R., Drtina, P. and Lang, E. (1999), "Numerical prediction of erosion on guide vanes and in labyrinth seals in hydraulic turbines", *Wear*, Vol. 2 Nos. 233-235, pp. 685-91.

Mendoza, C. and Zhou, D. (2001), "Turbulent intensities in open-channel flows", *Mechanics Research Communications*, Vol. 18, pp. 87-95.

Mitter, A., Malhotra, J.P. and Jadeja, H.T. (2004), "The two-fluid modeling of gas-particle transport phenomenon in confined systems considering inter particle collision effects", *International Journal of Numerical Methods for Heat and Fluid Flow*, Vol. 14, pp. 579-605.

Neelesh, K.J. and Vijaay, K.J. (2001), "Modeling of material removal in mechanical type advanced machining process: a state-of-art-review", *International Journal of Machine Tools and Manufacture*, Vol. 41, pp. 573-1635.

Paul, S., Hoogstrate, A.M., Lutterwelt, C.A. and Kals, H.J.J. (1998), "Analytical and experimental modeling of abrasive water jet cutting of ductile materials", *Journal of Materials and Processing Technolology*, Vol. 73, pp. 189-99.

Pei, Z.J. and Perreira, P.M. (1998), "Modeling of ductile mode material removal in rotary ultrasonic machining", *International Journal of Machine Tool Manufacture*, Vol. 38, pp. 1399-418.

Quercia, G., Grigorescu, I., Contreras, H., Di Rauso, C. and Gutierrez-Campos, D. (2001), "Friction and wear behavior of several hard materials", *International Journal of Refractory Metals*, Vol. 19, pp. 359-69.

Sommerfeld, M. (2003), "Analysis of collision effects for turbulent gas-particle flow in a horizontal channel", *International Journal of Multiphase Flow*, Vol. 12, pp. 121-34.

Sundaresan, S., Eaton, J., Koch, D.L. and Ottino, J.M. (2003), "Report of study group on disperse flow", *International Journal of Multiphase Flow*, Vol. 14, pp. 67-83.

Tabakoff, W. (1990), "Effect of environmental particles on a radial compressor", in Levy, A.V. (Ed.), *Proceedings on Corrosion-Erosion-Wear of Materials at Elevates Temperatures*, *Berkeley, CA*, pp. 261-8.

Tsuji, Y. (2000), "Activities in discrete particle simulation in Japan", *Powder Technology*, Vol. 113, pp. 278-86.

Wang, Z.Y. and Rajurkar, K.P. (1996), "Dynamic analysis of the ultrasonic machining process", *Transactions of ASME, Journal of Manufacturing Science and Engineering*, Vol. 118, pp. 376-81.

Corresponding author
Zdzislaw Mazur can be contacted at: mazur@iie.org.mx